Stable Metallic State of a Neutral-Radical Single-Component Conductor at Ambient Pressure

Yann Le Gal, Thierry Roisnel, Pascale Auban-Senzier, Nathalie Bellec, Jorge Íñiguez, Enric Canadell, Dominique Lorcy

Stable Metallic State of a Neutral Radical Single-Component Conductor at Ambient Pressure

Yann Le Gal,[1] Thierry Roisnel,[1] Pascale Auban-Senzier,[2] Nathalie Bellec,[1] Jorge Íñiguez,[3] Enric Canadell,*[4] and Dominique Lorcy*[1]

[1] *Univ Rennes, CNRS, ISCR (Institut des Sciences Chimiques de Rennes) - UMR 6226, F-35000 Rennes, France. E-mail: Dominique.lorcy@univ-rennes1.fr.*

[2] *Laboratoire de Physique des Solides UMR 8502 CNRS-Université de Paris-Sud, Bat 510, F-91405 Orsay cedex, France.*

[3] *Materials Research and Technology Department, Luxembourg Institute of Science and Technology (LIST),5 Avenue des Hauts-Fourneaux, L-4362 Esch/Alzette, Luxembourg.*

[4] *Institut de Ciència de Materials de Barcelona (ICMAB-CSIC), Campus de la UAB, E-08193 Bellaterra, Spain.*

ABSTRACT

Molecular metals have been essentially obtained with tetrathiafulvalene (TTF) based precursors, either with multi-component ionic materials or in a few instances in single-component systems. In that respect, gold bis(dithiolene) complexes, in their neutral radical state, provide a prototype platform toward such single component conductors. Herein we report the first single component molecular metal under ambient pressure derived from such Au complexes without any TTF backbone. This complex exhibits a conductivity of 750 S.cm^{-1} at 300 K up to 3800 S.cm^{-1} at 4 K. First-principles electronic structure calculations show that the striking stability of the metallic state finds its origin in sizeable internal electron transfer from the SOMO-1 to the SOMO of the complex as well as in substantial interstack and interlayer interactions.

INTRODUCTION

The quest for metallic behavior at ambient pressure is still a real challenge in single-component molecular conductors. Indeed, most compounds, which have been synthesized with this goal in mind, exhibit semiconducting behavior at ambient pressure with eventually a metallic state stabilized only under pressure. The first exception concerns the nickel bis(dithiolene) complexes involving tetrathiafulvalene (TTF) dithiolate ligands, [Ni(tmdt)$_2$] (tmdt = trimethylene-tetrathiafulvalenedithiolate), described in 2001, which has knocked down the idea that molecular materials could only be metallic if they resulted from the association of two different chemical species.[1] The second and last example recently reported involves a zwitterionic TTF-extended dicarboxylate radical (TED).[2] All other single-component systems reported so far exhibit to the best a metallic behavior only under high pressure, as for example the catechol-fused ethylenedithio-TTF (H$_2$Cat-EDT-TTF).[3] It should also be noted that all these systems have in common the presence of a TTF skeleton which provides an extensive delocalization.[4,5,6] Besides these TTF-based single-component conductors, all other investigated molecules are neutral radical species such as bis(dithiazolyl) derivatives,[7,8] or spiro-bis(phenalenyl)boron[9] or gold bis(dithiolene) complexes.[10,11,12,13] One intrinsic difficulty with such neutral radical species is their propensity to dimerize in the solid state. Even when dimerization does not take place, another challenge for stabilizing the metallic state is to increase the electronic bandwith W (which is generally narrow due to weak intermolecular interactions of the radicals in the solid state) over the onsite Coulomb repulsion U.[14] Thus, the conducting properties can be strongly influenced by the solid state packing and the strength of the intermolecular interactions. Therefore, minor changes performed on the skeleton of one or the other family mentioned above can greatly modify the outcome of this W/U competition.
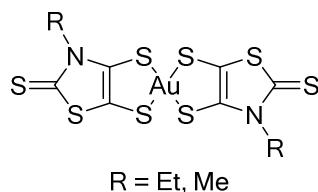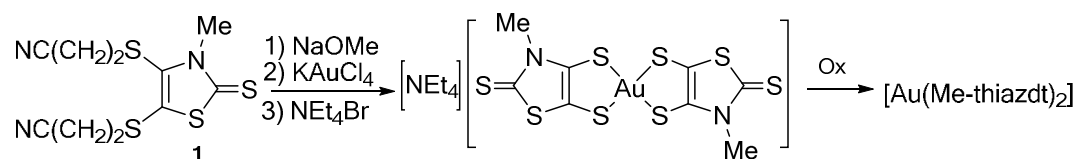
2

R = Et, Me

Chart 1. Chemical structures of the gold bis(dithiolene) complexes [Au(R-thiazdt)$_2$]

For our part, we previously reported a neutral gold dithiolene complex, [Au(Et-thiazdt)$_2$] (Chart 1), based on the *N*-ethyl-1,3-thiazoline-2-thione-4,5-dithiolate (Et-thiazdt) ligand which exhibits an activated conductivity of 0.33 S.cm^{-1} under ambient conditions but becomes metallic under a pressure of 1.3 GPa.[15,16] Different structural modifications of the ligand skeleton were investigated to stabilize the metallic state. For instance, substitution of selenium atoms for the sulfur atoms within the metallacycles increases the conductivity by two orders of magnitude and the metallic behavior is then reached already at 0.6 GPa, a consequence of increased intermolecular interactions and band dispersion in the solid state.[17] Introduction of bulkier groups than the ethyl one, such as propyl or isopropyl on the nitrogen atoms of the thiazole cores, induced completely different solid state organizations of the complexes with however similar room temperature conductivity values and activated behavior at ambient pressure. [18] Nevertheless, no insulator-to-metal transition was observed, a consequence of an original avoided band crossing which strongly stabilized the non-metallic behavior.[19] All these structural modifications gave us a better understanding of the structure-properties relationship on this single-component-conductor family. These earlier investigations prompted us to analyze another member of this gold bis(dithiolene) complex belonging to the same [Au(R-thiazdt)$_2$] family, but with now a smaller substituent on the nitrogen atoms, *i. e.* the methyl group. This modification is expected to bring closer to each other the radical complexes in the solid state and thus to favor larger band dispersion (W) to eventually stabilize a metallic state. Our previous experiences with this methyl-substituted

ligand (Me-thiazdt) in its Ni and Pd complexes have shown some drawbacks.[20] Indeed, these complexes are not only poorly soluble but they also exhibit a recurrent S/N-Me disorder due to the dissymmetry of the ligand. Such disorder would be strongly unfavourable to stabilize the metallic state. However, we decided to investigate the corresponding neutral radical gold complex, [Au(Me-thiazdt)$_2$]$^{\bullet}$, taking into account that in all the neutral species studied so far with R $\neq$ Me only one isomer was isolated. Herein, we report the synthesis, crystal structure and electronic properties of the single-component molecular conductor formulated as [Au(Me-thiazdt)$_2$]$^{\bullet}$ which exhibits for the first time metallic behavior under ambient pressure, in the whole temperature range down to 4K.

RESULTS AND DISCUSSION

The monoanionic gold bis(dithiolene) complex [Au(Me-thiazdt)$_2$]$^{-1}$ was synthesized as the Et$_4$N^{+} salt starting from the cyanoethylthio protected dithiolene ligand **1**[20] according to the previously reported method (Scheme 1).[15,17,19,20] Black crystals were obtained by recrystallization in acetonitrile.

Scheme 1 Synthesis of the neutral radical gold complex [Au(Me-thiazdt)$_2$]$^{\bullet}$

As shown in Figure 1, each dithiolene ligand is actually disordered on two positions as feared. This disorder has been previously observed on Ni and Pd bis(dithiolene) complexes using the same dissymmetrical ligand.[20] It is worth mentioning that when the substituent on the nitrogen

4

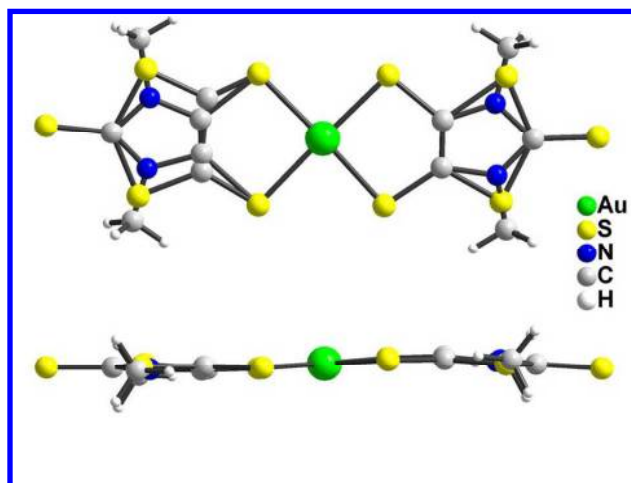atom is bigger than a methyl group no disorder was observed and the *trans* isomer was obtained.[15,17,18,19]

Figure 1. Molecular view of the [Au(Me-thiazdt)$_2$]$^{-1}$ complex in [NEt$_4$][Au(Me-thiazdt)$_2$] (top) and side view (bottom).

Preparative oxidation of [NEt$_4$][Au(Me-thiazdt)$_2$] has been performed by electrocrystallization upon application of a constant current intensity of 0.4 µA in the presence of NBu$_4$PF$_6$ as the supporting electrolyte in CH$_3$CN. Using these conditions, black crystals were collected at the anode after 15 days. The neutral radical [Au(Me-thiazdt)$_2$]$^\bullet$ is fully planar and crystallizes as the *trans* isomer only. In the solid state, the gold complexes form uniform stacks along the *b* axis with a mean plane-to-plane distance of 3.51 Å (Figure 2a and 2b) . The overlap between molecules along the stacks is characterized by a lateral slip between neighboring complexes with short S•••S contacts of 3.727 Å (Figure 2c). Between the stacks, several shorter S•••S intermolecular contacts are also observed (Figure 2d), to give a 2D character. This organization is reminiscent to that described for the ethyl compound, [Au(Et-thiazdt)$_2$]. However, in [Au(Me-thiazdt)$_2$]$^\bullet$ all the intermolecular S•••S contacts are notably shorter. Moreover, in the *ac* plane (Figure 2a), an additional S•••S intermolecular contact is observed between the exocylic sulfur atom of the complexes at 3.567(8) Å,

5

connecting the (*bc*) slabs in the third direction. This additional S•••S contact was not observed
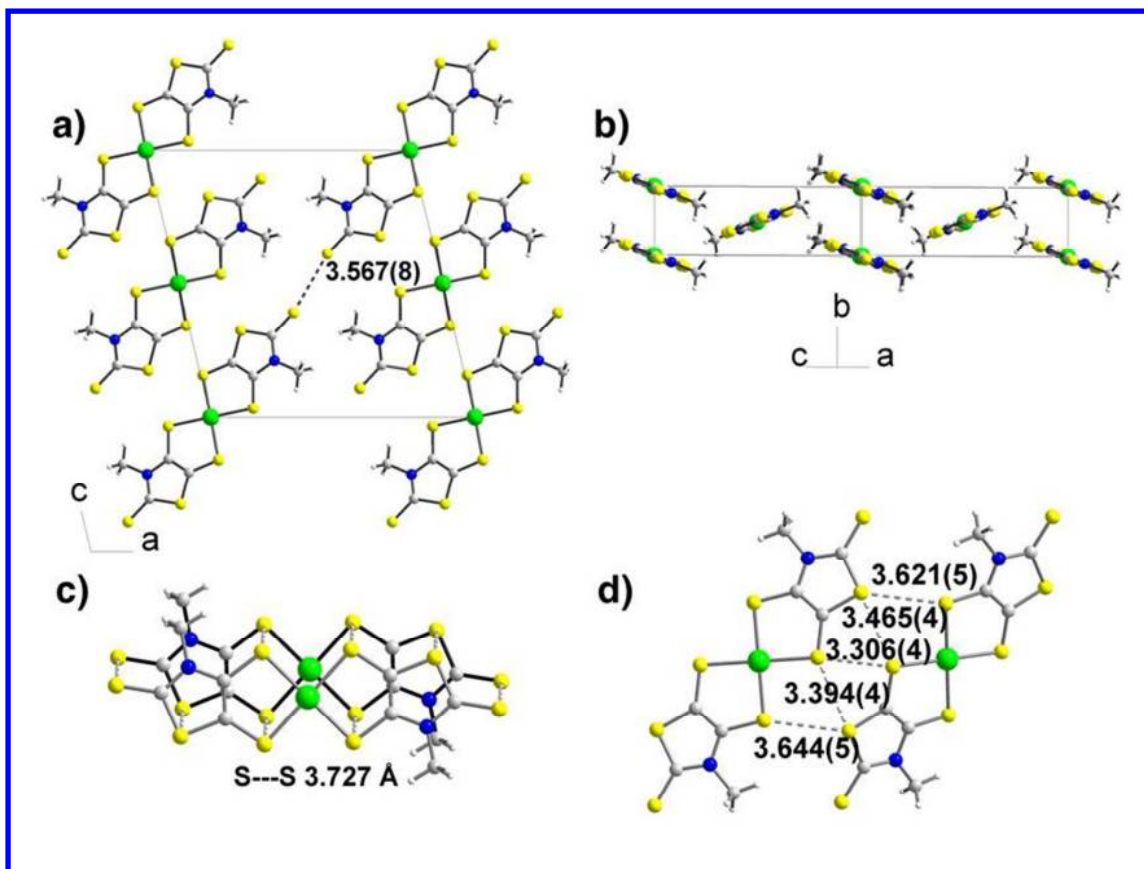
in [Au(Et-thiazdt)$_2$].

Figure 2. (a) Projection view along *b* of the unit cell of [Au(Me-thiazdt)$_2$]$^{\bullet}$, (b) detail of the

stacking along *b*, (c) detail of the intra-stack overlap, and (d) view of the short S•••S contacts

between neighboring stacks of [Au(Me-thiazdt)$_2$]$^{\bullet}$.

The electrical resistivity was measured on single crystals along the *b* axis (long axis of the

needle). At room temperature and ambient pressure, the conductivity is around 750 S.cm^{-1}

which is about 2300 times higher than the conductivity reported for the ethyl substituted

complex [Au(Et-thiazdt)$_2$]. It is actually the highest conductivity measured under ambient

conditions in any single component molecular conductor. The temperature dependence of the

conductivity is reported in Figure 3. Upon cooling, a metallic behavior is observed in the

whole temperature range from 300 to 4 K with a ratio of 5 between these two temperatures.

6

The compound exhibits a weak temperature independent paramagnetism together with a small Curie-type contribution not exceeding 0.2% of $S = 1/2$ species. This Pauli-type susceptibility amounts to 3.2×10^{-4} emu/mol, a value in line with the metallic character of this single-component conductor (Figure 3). This susceptibility value is similar to that found for the single-component molecular conductors based TTF,[1,2] bis(dithiazolyl) derivatives[7,8] and spiro-bis(phenalenyl)boron[9] as well as for highly conducting multi component systems based on metal dithiolene complexes.[21]

Figure 3. Temperature dependence of the conductivity of $[Au(Me\text{-}thiazdt)_2]^{\bullet}$ with the magnetic susceptibility in the inset.

In order to understand the origin of the metallic behavior of the present system we have carried out first-principles density functional theory (DFT) calculations with exactly the same settings used in our previous studies of single-component molecular conductors of the $[Au(Et\text{-}thiazdt)_2]$ family.[15,17] We first investigated the nature of the ground state using the experimental crystal structure and a double unit cell along the b-direction (i.e. containing four molecules, two along the chains direction, b, and two along the interchains direction, c). Such double unit cell allowed us to carry out calculations for the metallic and several localized

states where all possibilities of ferromagnetic (FM) and antiferromagnetic (AFM) orderings along both the *b*- and *c*-directions were considered. In stark contrast with the previously studied systems of the [Au(Et-thiazdt)$_2$] family,[15,17] the ground state of the system was found to be a paramagnetic metallic state, in excellent agreement with our transport measurements.

The calculated band structure using the crystallographic cell (i.e. containing two molecules) is reported in Figure 4a. Such band structure contains two pairs of dispersive bands cut by the Fermi level (at 0 eV) which are at the origin of the non-activated metallic behavior. As for the other conductors of this family, the upper and lower of these pairs of bands originate from the singly occupied molecular orbital (SOMO) and the orbital immediately below (SOMO-1) of the complex (Figure 4b).[15,17] Since the energy difference between the SOMO and SOMO-1 is of the same order as the intermolecular transfer integrals, the two pairs of bands overlap and both become partially filled,[21,22,23] in contrast with the situation in the isolated complex. These bands exhibit an almost cosine-like shape along the chains direction (Γ-Y) except for the upper SOMO band which near the region of the Γ point undergoes an avoided crossing with a low-lying empty band. However, since this feature occurs above the Fermi level and does not have significant implications for the present work, it will not be further discussed.

To understand the origin of the stable metallic properties of this system we must answer the two following questions: (i) what distinguishes this system from the previously reported ones of this family which are localized and only under pressure lead to metallic behavior?, and (ii) why, even if exhibiting a noticeable pseudo-1D band structure, is the system immune to the usual charge or spin density wave electronic instabilities destroying the metallic state in low-dimensional systems?
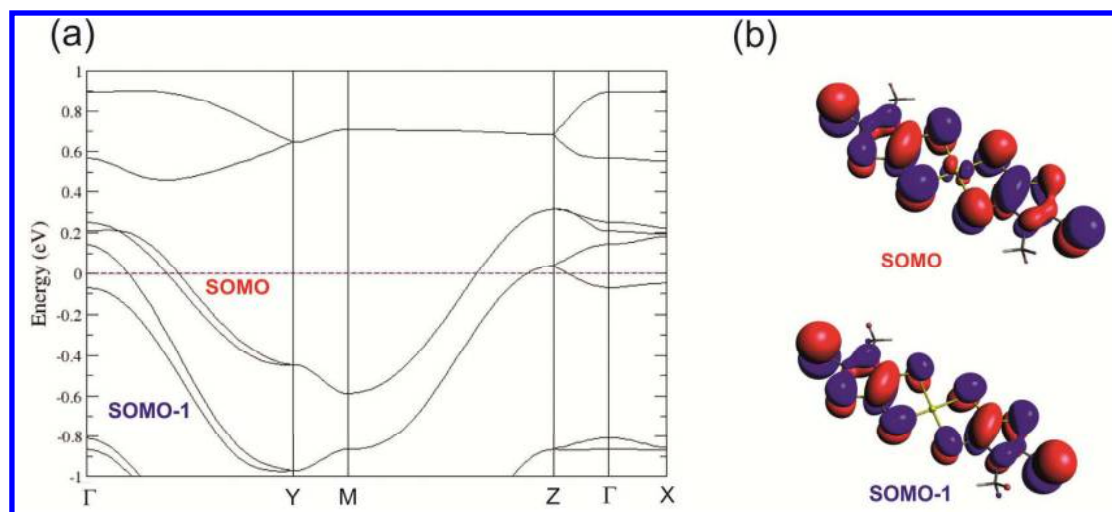
Figure 4. (a) Calculated band structure for the metallic state of [Au(Me-thiazdt)$_2$]$^{\bullet}$ where the dotted purple line refers to the Fermi level. Γ, Y, Z, M and X refer to the (0, 0, 0), (0, 1/2, 0), (0, 0, 1/2), (0, 1/2, 1/2) and (1/2, 0, 0) points of the monoclinic Brillouin zone. (b) Nature of the SOMO and SOMO-1 levels of [Au(Me-thiazdt)$_2$]$^{\bullet}$.

Let us first consider the question of the localized *vs* metallic nature of the ground state. for these gold bis(dithiolene) complexes. In Figure 5a we report the band structure for the AFM ground state of [Au(Et-thiazdt)$_2$].[15] Since an AFM state along the chains implies a double cell along this direction (i.e. a total of four complexes), the band structure of Figure 5a contains four SOMO and four SOMO-1 bands. The key aspect of this figure is the presence of a small band gap separating the highest pair of SOMO bands from the lower ones. The occurrence of this small gap is responsible for the activated resistivity behavior at ambient pressure. Since only half of the SOMO bands are filled in this band structure, the SOMO level of the different complexes contains only one electron, as in the isolated complex. Thus, the band structure of Figure 5a is just the electronic description of a set of [Au(Et-thiazdt)$_2$] radicals coupled antiferromagnetically along the chains. Figure 5b shows the band structure of the present [Au(Me-thiazdt)$_2$]$^{\bullet}$ system (Figure 4a) when plotted using a double cell exactly as for [Au(Et-thiazdt)$_2$]. It is simply a folded version along the chains direction of the original

one (for a detailed description of the connection between the two band structures and the gap

opening due to the AFM correlations we refer the reader to our previous work on [Au(Et-

thiazdt)$_2$][15]). As mentioned, the key feature in stabilizing the AFM ground state of [Au(Et-

thiazdt)$_2$] and other members of the family previously reported is the development of a band

gap in the regions around the Y and M points as a result of the AFM correlations, which

effectively separate the upper pair of bands from the lower lying ones. These gaps are of the

order of ~0.1 eV. Coming back to the band structure of Figure 5b it is clear that band gaps

between two and three times larger than in [Au(Et-thiazdt)$_2$] should develop around the M and

Y points to suppress the metallic conductivity by the same mechanism (see green arrows in

Figure 5b). This is too large for such a mechanism to be a likely alternative; even in that case

it would not be clear whether the gap would really occur, because now the upper SOMO-1

band at Γ (around -0.26 eV) is not well separated from the lower SOMO band. As a

consequence of non-negligible interlayer interactions this band practically overlaps with the

upper SOMO bands along the interlayer direction (the Γ – X line in Figure 5b). Thus, the

development of a gap because of AFM correlations is not a likely alternative for the present

system. The larger dispersion of both the SOMO and SOMO-1 bands compared with the other

members of the family lies at the origin of this remarkable feature. According to our

calculations replacement of a methyl for an ethyl group leads practically to a doubling of the

SOMO and SOMO-1 band dispersions. From a structural viewpoint such effect finds its roots

in the shortening of the S•••S interactions associated with the inner sulfur atoms of the present

system (3.727 vs. 3.841 Å in [Au(Et-thiazdt)$_2$]$^•$ along the chain direction; 3.306 and 3.394 Å

vs. 3.419 and 3.528 Å in [Au(Et-thiazdt)$_2$]$^•$ between neighboring stacks; see the structral
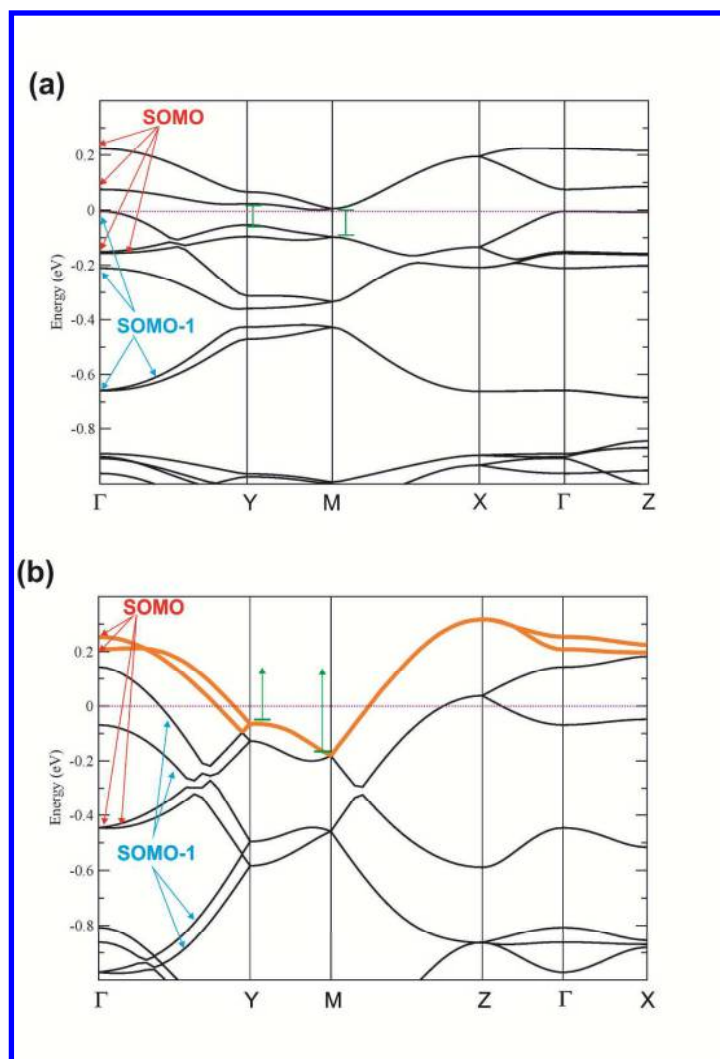
discussion and Figure 2).

Figure 5. Calculated band structure for the ground states of [Au(Et-thiazdt)$_2$]$^{\bullet}$ (a) and [Au(Me-thiazdt)$_2$]$^{\bullet}$ (b) using a double cell along the chains direction, *b*. The dotted line in (a) refers to the highest occupied level. Γ, Y, Z and X refer to the (0, 0, 0), (0, 1/2, 0), (0, 0, 1/2) and (1/2, 0, 0) points of a monoclinic Brillouin zone with *b'* = 2*b*; M refers to (1/2, 1/2, 0) in (a) and to (0, 1/2, 1/2) in (b). Note that the layers occur in the (*ab*) plane for [Au(Et-thiazdt)$_2$]$^{\bullet}$ but in the (*bc*) plane for [Au(Me-thiazdt)$_2$]$^{\bullet}$.

A complementary way to understand the preference for the metallic state is to notice that, because of the larger overlap of the SOMO and SOMO-1 bands there is an effective transfer of electrons from the SOMO-1 to the SOMO levels. According to the present

calculations this transfer is as large as 0.16 electrons per gold bis(dithiolene) complex. The SOMO and SOMO-1 levels of the present system thus contain $(1 + \delta)$ and $(2 - \delta)$ electrons with $\delta = 0.16$, which is very far from the case of the isolated radical ($\delta = 0$) or the hypothetical metallic state of $[Au(Et\text{-}thiazdt)_2]$ ($\delta \approx 0$) for which the AFM ordering of neutral radicals is favored. In other words, the stronger SOMO•••SOMO and SOMO-1•••SOMO-1 interactions brought about by the shorter inner S•••S contacts lead to the creation of too large a number of electrons and holes in the SOMO and SOMO-1 levels of the complex which prefer to delocalize imposing a non-activated metallic conductivity. When $\delta \approx 0$ the gold bis(dithiolene) complexes prefer to retain the SOMO unpaired electron ultimately leading to the localized state and activated conductivity behavior.
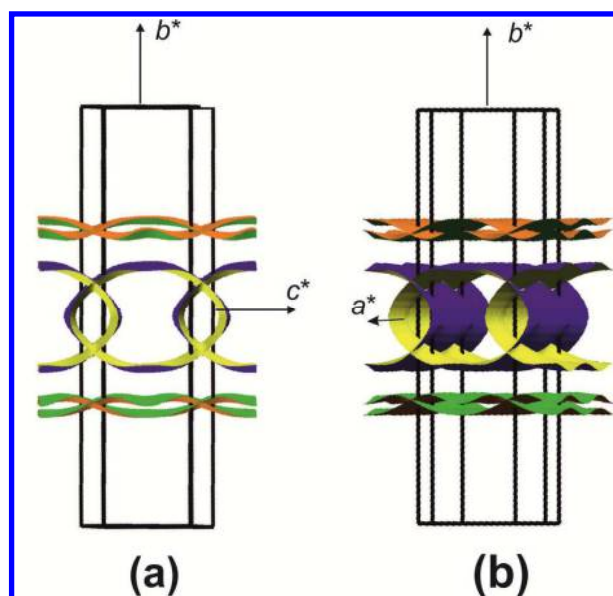

Figure 6. Calculated Fermi surface for $[Au(Me\text{-}thiazdt)_2]^{\bullet}$: (a) view perpendicular to the layers (i.e. along the a^*-direction) and (b) a view somewhat rotated around b^*.

We now must understand why the metallic system is robust with respect to hypothetical electronic instabilities due to nesting of the Fermi surface which frequently occur in low-dimensional materials.[24,25] For this we must focus on the nature of Fermi surface (see Figure 6a and 6b). Shown in Figure 6a is a view perpendicular to the layers of [Au(Me-thiazdt)$_2$]$^{\bullet}$, i.e. along a^*. The upper and lower pair of warped planes originate from the SOMO bands; the overlapping cylinders with elliptical cross-section parallel to the a^*-direction originate from the SOMO-1 bands. [Au(Me-thiazdt)$_2$]$^{\bullet}$ is thus predicted to be a 2D metal with better conductivity along the chains axis, b. Being closed, the SOMO-1 component does not exhibit nesting properties which could lead to a charge or spin modulation destroying this portion of the Fermi surface. As mentioned above, in contrast with all other members of the family of the [Au(Et-thiazdt)$_2$] molecular solids,[15,17] there are substantial intermolecular interactions along the interlayer a^*-direction leading to the non-negligible dispersion of the bands along this line ($\Gamma - X$ in Figure 4a). This is obviously the result of the stronger interlayer contacts brought about by the smaller size of the substituent (see for instance the S•••S contact of 3.567 Å in Figure 2a, which does not occur in other salts of this family). The joint effect of the warping along the interchain (c) and interlayer (a^*) directions due to these S•••S interactions leads to a considerable corrugation of the SOMO portion of the Fermi surface, i.e. the two upper and lower pairs of pseudo planes of Figure 6b. Because of this corrugation, the possible nesting of the SOMO contribution seriously deteriorates and there is no tendency towards the usual instability of low-dimensional systems with open Fermi surface.[24] It is important to note that, even if such instability occurred, the cylindical portion would not be destroyed by the modulation and the metallic character would be kept.[26]

CONCLUSION

In summary, the smaller size of the methyl substituent, on this gold bis(dithiolene) complex, stabilizes the metallic state by leading to stronger intermolecular interactions which impose: (i) a sizeable internal electron transfer creating an important number of holes and electrons in the SOMO-1 and SOMO levels and, (ii) closed or substantially corrugated Fermi surface contributions for the SOMO-1 and SOMO levels respectively. The joint action of the two effects leads to the highly stable metallic ground state for $[Au(Me-thiazdt)_2]^{\bullet}$.

EXPERIMENTAL SECTION

Chemicals and materials from commercial sources were used without further purification. The thiazoline-2-thione **1** was prepared according to the literature.[20]

Synthesis of [NEt$_4$][Au(Me-thiazdt)$_2$] To a dry two necked flask containing thiazoline-2-thione **1** (125 mg, 0.42 mmol) was added a solution of NaOMe (3.4 mmol) in dry methanol (prepared from 77 mg of Na in 10 mL of dry MeOH) under inert atmosphere. The solution was stirred 1 hour and a solution of KAuCl$_4$ (96 mg, 0.25 mmol) in 15 mL of dry MeOH was added. The reaction mixture was stirred 5 hours at room temperature and NEt$_4$Br (133 mg, 0.63 mmol) was added. The mixture was stirred at room temperature for 24 hours and the precipitate was filtered and recrystallized in Me$_3$CN to afford [NEt$_4$][Au(Me-thiazdt)$_2$] as dark crystals. Yield 29 %. Mp 225°C; ^{1}H NMR (300MHz, (CD$_3$CN) δ 1.23 (m, 12H, CH$_3$), 3.18 (q, 8H, CH$_2$, J = 7.3 Hz), 3.51 (s, 6H, CH$_3$); ^{13}C NMR (75 MHz, (CD$_3$)$_2$SO) δ 7.5 (CH$_3$-CH$_2$), 34.4 (CH$_3$), 51.9 (CH$_2$), 110.1 (C=C), 132.3 (C=C), 191.2 (C=S); HRMS (ESI) calcd for [2C$^+$, A$^-$]$^+$ C$_{24}$H$_{46}$N$_4$S$_8$Au: 843.11538. Found: 843.1159; Anal. calcd for C$_{16}$H$_{26}$AuN$_3$S$_8$: C, 26.92; H 3.67; N, 5.89; S 35.93. Found: C, 26.94; H 3.78; N, 5.88; S 36.39.

Electrocrystallization. Crystals of $[Au(Me-thiazdt)_2]^{\bullet}$ were prepared electrochemically using a standard H-shaped cell (12 mL) with Pt electrodes. An acetonitrile solution of

[NEt$_4$][Au(Me-thiazdt)$_2$] (10 mg) was placed in the anodic compartment, and Bu$_4$NPF$_6$ (100 mg) in both compartments. Black needle crystals of [Au(Me-thiazdt)$_2$]$^•$ suitable for X-ray diffraction studies, were obtained on the anode upon application of a constant current of 0.4 μA for 15 days.

Crystallography. Single-crystal diffraction data were collected on APEXII for [NEt$_4$][Au(Me-thiazdt)$_2$] and on D8 VENTURE for [Au(Me-thiazdt)$_2$], Bruker-AXS diffractometer, Mo-Kα radiation (λ = 0.71073 Å) for all compounds. For [NEt$_4$][Au(Me-thiazdt)$_2$] the structure was solved by dual-space algorithm using the *SHELXT* program[27] and for [Au(Me-thiazdt)$_2$] the structure was solved by direct methods using the *SIR97* program[28], and then refined with full-matrix least-square methods based on F^2 (*SHELXL-97*).[29] All non-hydrogen atoms were refined with anisotropic atomic displacement parameters. H atoms were finally included in their calculated positions. Details of the final refinements are given in Table S1.

Resistivity measurements. The resistivity measurements were performed along the long axis of the needles (*b* crystallographic axis) of [Au(Me-thiazdt)$_2$]. Gold pads were evaporated on the crystals in order to improve the quality of the contacts and gold wires were glued with silver paste on these contacts. Then a standard four points technique was used with a low frequency lock-in detection (I$_{ac}$ = 10 μA). Low temperature was provided by a homemade cryostat equipped with a 4 K pulse-tube.

Magnetic measurements. The magnetic susceptibility measurements were performed in a Quantum Design SQUID magnetometer MPMS-XL. Measurements were realized on 13.2 mg of polycrystalline samples of [Au(Me-thiazdt)$_2$] under a magnetic field of 5000 G in the temperature range 1.8-300K. The magnetization data were corrected for the sample holder and the diamagnetic contributions.

Computational details. We have carried out both spin-polarized and non spin-polarized calculations using the Generalized Gradient Approximation [30] to Density Functional Theory[31,32] (DFT) as implemented in the *Vienna Ab Initio Simulation Package* (VASP).[33] We used the Projector Augmented Wave [34,35] method to represent the ionic cores, solving explicitly for the following electrons: $5d$ and $6s$ of Au, $3s$ and $3p$ of S, $2s$ and $2p$ of N and C, and $1s$ of H. Electronic wave functions were represented with a plane wave basis truncated at 400 eV. Γ-centered $4{\times}8{\times}4$ k-point grids for the simulation cell with 4 molecules were used to converge the calculations. The Fermi surfaces were plotted by interpolating a four orbital tight-binding Hamiltonian computed from our DFT results using the maximally localized Wannier function (MLWF) method[36,37] as implemented in the wannier90 code.[38]

Supporting Information

X-ray crystallographic files in CIF format and cyclic voltammogram of [NEt$_4$][Au(Me-thiazdt)$_2$]. This material is available free of charge via the Internet at http://pubs.acs.org.

Acknowledgments

Competing financial Interest

The authors declare no competing financial interest.

References

[1] (a) Tanaka, H.; Okano, Y.; Kobayashi, H.; Suzuki, W.; Kobayashi, A. A three-dimensional synthetic metallic composed of single-component molecules. *Science* **2001**, *291*, 285–287. (b) Kobayashi, A.; Fujiwara, E.; Kobayashi, H. Single-component molecular metals with extended-TTF dithiolate ligands. *Chem. Rev.* **2004**, *104*, 5243−5264. (c) Cui, H.; Kobayashi, H.; Ishibashi, S.; Sasa, M.; Iwase, F.; Kato, R.; Kobayashi, K. A single-component molecular superconductor. *J. Am. Chem. Soc.* **2014**, *136*, 7619−7622.

[2] Kobayashi, Y.; Terauchi, T.; Sumi, S.; Matsushita, Y. Carrier generation ans electronic properties of a single-component pure organic metal. *Nat. Mater.* **2017**, *16*, 109-114.

[3] Isono, T.; Kamo, H.; Ueda, A.; Takahashi, K.; Nakao, A.; Kumai, R.; Nakao, H.; Kobayashi, K.; Murakami, Y.; Mori, H. Hydrogen bond-promoted metallic state in a purely organic single-component conductor under pressure. *Nat. Commun.* **2013**, *4*, 1344–1349.

[4] Ferraris, J.; Cowan, D. O.; Walatka, V.; Perlstein, J. H. Electron transfer in a new highly conducting donor-acceptor complex. *J. Am. Chem. Soc.* **1973**, *95*, 948−949.

[5] Williams, J. M.; Schultz A. J.; Geiser U.; Carlson, K. D.; Kini, A. M.; Wang, H. H.; Kwok, W. K.; Whangbo, M. H.; Schirber, J. E. Organic superconductors—new benchmarks. *Science* **1991**, *252*, 1501–1508.

[6] Coronado, E.; Galan-Mascaros, J. R.; Gomez-Garcia, C. J.; Laukhin, V. Coexistence of ferromagnetism and metallic conductivity in a molecule-based layered compound. *Nature* **2000**, *408*, 447–449.

[7] Mailman, A.; Wong, J. W. L.; Winter, S. M.; Claridge, R. C. M.; Robertson, C. M.; Assoud, A.; Yong, W.; Steven, E.; Dube, P. A.; Tse, J. S.; Desgreniers, S.; Secco, R. A.; Oakley, R. T. Fine tuning the performance of multiorbital radical conductors by substituent effects. *J. Am. Chem. Soc.* **2017**, *139*, 1625–1635.

[8] (a) Tian, D.; Winter, S. M.; Mailman, A.; Wong, J. W. L.; Yong, W.; Yamaguchi, H.; Jia, Y.; Tse, J. S.; Desgreniers, S.; Secco, R. A.; Julian, S. R.; Jin, C.; Mito, M.; Ohishi, Y.; Oakley, R. T. The metallic state in neutral radical conductors: dimensionality, pressure and multiple orbital effects. *J. Am. Chem. Soc.* **2015**, *137*, 14136–14148. (b) Wong, J. W. L.; Mailman, A.; Lekin, K.; Winter, S. M.; Yong, W.; Zhao, J.; Garimellas, S. V.; Tse, J. S.; Secco, R. A.; Desgreniers, S.; Ohishi, Y.; Borondics, F.; Oakley, R. T. Pressure induced phase transitions and metallization of a neutral radical conductor. *J. Am. Chem. Soc.* **2014**, *136*, 1070–1081. (c) Mailman, A.; Winter, S. M.; Yu, X.; Robertson, C. M.; Yong, W.; Tse, J. S.; Secco, R. A.; Liu, Z.; Dube, P. A.; Howard, J. A. K.; Oakley, R. T. Crossing the insulator-to-metal barrier with a thiazyl radical conductor. *J. Am. Chem. Soc.* **2012**, *134*, 9886–9889. (d) Yu, X.; Mailman, A.; Lekin, K.; Assoud, A.; Robertson, C. M.; Noll, B. C.; Campana, C. F.; Howard, J. A. K.; Dube, P. A.; Oakley, R. T. Semiquinone-bridged bisthiazolyl radical as neutral radical conductors. *J. Am. Chem. Soc.* **2012**, *134*, 2264–2275.

[9] (a) Pal, S. K.; Itkis, M. E.; Tham, F. S.; Reed, R. W.; Oakley, R. T.; Haddon, R. C. Resonating valence-bond ground state in a phenalenyl-based neutral radical conductor. *Science* **2005**, *309*, 281–284. (b) Mandal, S.; Samanta, S.; Itkis, M. E.; Jensen, D. W.; Reed, R. W.; Oakley, R. T.; Tham, F. S.; Donnadieu, B.; Haddon, R. C. Resonating valence bond ground state in oxygen-functionalized phenalenyl-based neutral radical molecular conductors. *J. Am. Chem. Soc.* **2006**, *128*, 1982–1994. (c) Pal, S. K.; Bag, P.; Itkis, M. E.; Tham, F. S.; Haddon, R. C. Enhanced electrical conductivity in a

substitutionally doped spiro-bis(phenalenyl)boron radical molecular solid. *J. Am. Chem. Soc.* **2014**, *136*, 14738−14741.

[10] Schiødt, N. C.; Bjørnholm, T.; Bechgaard, K.; Neumeier, J. J.; Allgeier, C.; Jacobsen, C. S.; Thorup, N. Structural, electrical, magnetic, and optical properties of bis-benzene-1,2-dithiolato-Au(IV) crystals. *Phys. Rev. B* **1996**, *53*, 1773-1778.

[11] Belo, D.; Alves, H.; Lopes, E. B.; Duarte, M. T.; Gama, V.; Henriques, R. T.; Almeida, M.; Pérez-Benítez, A.; Rovira, C.; Veciana, J. Gold complexes with dithiothiophene digands: A metal based on a neutral molecule. *Chem. Eur. J.* **2001**, *7*, 511−519.

[12] Dautel, O. J.; Fourmigué, M.; Canadell, E.; Auban-Senzier, P. Fluorine segregation controls the solid-state organization and electronic properties of Ni and Au dithiolene complexes: stabilization of a conducting single-component gold dithiolene complex. *Adv. Funct. Mater.* **2002**, *12*, 693−698.

[13] Branzea, D. G.; Pop, F.; Auban-Senzier, P.; Clérac, R.; Alemany, P.; Canadell, E.; Avarvari, N. Localization versus delocalization in chiral single component conductors of gold bis(dithiolene) complexes. *J. Am. Chem. Soc.* **2016**, *138*, 6838–6851.

[14] Mott N. F. Metal-insulator transitions. 2nd ed. London, UK: Taylor & Francis 1990.

[15] Tenn, N.; Bellec, N.; Jeannin, O.; Piekara-Sady, L.; Auban-Senzier, P.; Íñiguez, J.; Canadell, E.; Lorcy, D. A single-component molecular metal based on a thiazole dithiolate gold complex. *J. Am. Chem. Soc.* **2009**, *131*, 16961–16967.

[16] (a) Brière, B.; Caillaux, J.; Le Gal, Y.; Lorcy, D.; Lupi, S.; Perucchi, A.; Zaghrioui, M.; Soret, J. C.; Sopracase, R.; Ta Phuoc, V. Interplay between bandwidth-controlled and filling-controlled pressure-induced Mott insulator to metal transition in the molecular compound [Au(Et-thiazdt)$_2$]. *Phys. Rev. B* **2018**, *97*, 035101. (b) Stoliar, P.; Diener, P.; Tranchant, J.; Corraze, B.; Brière, B.; Ta-Phuoc, V.; Bellec, N.; Fourmigué, M.; Lorcy, D.;

Janod, E.; Cario, L. Resistive switching induced by electric pulses in a single-component molecular Mott insulator. *J. Phys. Chem. C* **2015**, *119*, 2983–2988.

[17] Yzambart, G.; Bellec, N.; Nasser, G.; Jeannin, O.; Roisnel, T.; Fourmigué, M.; Auban-Senzier, P.; Íñiguez, J.; Canadell, E.; Lorcy, D. Anisotropic chemical pressure effects in single-component molecular metals based on radical dithiolene and diselenolene gold complexes. *J. Am. Chem. Soc*. **2012**, *134*, 17138–17148.

[18] Filatre-Furcate, A.; Roisnel, T.; Fourmigué, M.; Jeannin, O.; Bellec, N.; Auban-Senzier, P.; Lorcy, D. Subtle steric differences impact the structural and conducting properties of radical gold bis(dithiolene) complexes. *Chem. Eur. J.* **2017**, *23*, 16004–16013.

[19] Filatre-Furcate, A.; Bellec, N.; Jeannin, O.; Auban-Senzier, P.; Fourmigué, M.; Íñiguez, J.; Canadell, E.; Brière, B.; Lorcy, D. Single-component conductors: a sturdy electronic structure generated by bulky substituents. *Inorg. Chem.* **2016**, *55*, 6036–6046.

[20] Eid, S.; Fourmigué, M.; Roisnel, T.; Lorcy, D. Influence of the thiazole backbone on the structural, redox, and optical properties of dithiolene and diselenolene complexes. *Inorg. Chem*. **2007**, *46*, 10647–10654.

[21] (a) Kato, R. Development of π-electron systems based on [M(dmit)$_2$] (M= Ni and Pd; dmit: 1,3-dithiole-2-thione-4,5-dithiolate) anion radicals. *Bull. Chem. Soc. Jpn*. **2014**, *87*, 355−374. (b) Kato, R. Conducting metal dithiolene complexes: Structural and electronic properties. *Chem. Rev.* **2004**, *104*, 5319−5346.

[22] Canadell, E.; Rachidi, I. E.-I.; Ravy, S.; Pouget, J.-P.; Brossard, L.; Legros, J.-P. On the band electronic structure of X [M (dmit)$_2$]$_2$ (X = TTF, (CH$_3$)$_4$N ; M = Ni, Pd) molecular conductors and superconductors. *J. Phys. (France)* **1989**, *50*, 2967−2981.

[23] Canadell, E. Electronic structure of two-band molecular conductors. *New. J. Chem*. **1997**, *21*, 1147-1159.

[24] Jérome, D.; Schulz, H. J. Organic conductors and superconductors. *Adv. Phys*. **1982**, *31*, 299−490.

[25] Canadell, E.; Whangbo, M.-H. Conceptual aspects of structure-property correlations and electronic instabilities, with applications to low-dimensional transition-metal oxides. *Chem. Rev*. **1991**, *91*, 965-1034.

[26] Kaddour, W.; Auban-Senzier, P.; Raffy, H.; Monteverde, M.; Pouget, J.-P.; Pasquier, C. R.; Alemany, P.; Canadell, E.; Valade, L. Charge density wave and metallic state coexistence in the multiband conductor TTF[Ni(dmit)$_2$]2. *Phys. Rev. B* **2014**, *90*, 205132.

[27] Sheldrick G.M. SHELXT - Integrated space group and crystal structure determination. *Acta Cryst.* **2015**, *A71*, 3−8.

[28] Altomare, A.; Burla, M. C.; Camalli, M.; Cascarano, G.; Giacovazzo, C.; Guagliardi, A.; Moliterni, A. G. G.; Polidori, G.; Spagna, R. SIR97: a new tool for crystal structure determination and refinement. *J. Appl. Cryst.* **1999**, *32*, 115−119.

[29] Sheldrick G. M. Crystal structure refinement with SHELX. *Acta Cryst*. **2015**, *C71*, 3−8.

[30] Perdew, J. P.; Burke, K.; Ernzerhof, M. Generalized gradient approximation made simple. *Phys. Rev. Lett.* **1996**, *77*, 3865−3868.

[31] Hohenberg, P.; Kohn, W. Inhomogeneous electron gas. *Phys. Rev.* **1964**, *136*, B864−B871.

[32] Kohn, W.; Sham, L. J. Self-consistent equations including exchange and correlation effects. *Phys. Rev.* **1965**, *140*, A1133−A1138.

[33] Kresse, G.; Furthmuller, J. Efficient iterative schemes for *ab initio* total-energy calculations using a plane-wave basis set. *Phys. Rev. B* **1996**, *54*, 11169-11186.

[34] Blöchl, P. E. Projector augmented-wave method. *Phys. Rev B* **1994**, *50*, 17953-17979.

[35] Kresse, G.; Joubert, D. From ultrasoft pseudopotentials to the projector augmented-wave method. *Phys. Rev. B,* **1999**, *59*, 1758-1775.

[36] Marzari, N.; Vanderbilt, D. Maximally localized generalized Wannier functions for composite energy bands. *Phys. Rev. B*, **1997**, *56*, 12847–12865.

[37] Souza, I.; Marzari, N.; Vanderbilt, D. Maximally localized Wannier functions for entangled energy bands. *Phys. Rev. B* **2002**, *65*, 035109.

[38] Mostofi, A. A.; Yates, J. R.; Lee, Y.-S.; Souza, I.; Vanderbilt, D.; Marzari, N. Wannier90: a tool for obtaining maximally-localised Wannier functions. *Comput. Phys. Commun.* **2008**, *178*, 685–699.

Table of Contents Graphic